Oxygen intrusions sustain aerobic nitrite oxidation in anoxic marine zones

Pearse J. Buchanan[1,*], Xin Sun[1], JL Weissman[2,3], Emily Zakem[1].

[1]Carnegie Institute of Global Ecology, 260 Panama Ave, Stanford, 94305, California, USA.
[2]Department of Biological Sciences-Marine and Environmental Biology, University of Southern California, Los Angeles, California, 90089, USA.
[3]Schmid College of Science and Technology, Chapman University, Orange, CA, 92866, USA.

**Correspondence to*: Pearse J. Buchanan (pbuchanan@carnegiescience.edu)

Abstract

Anoxic marine zones (AMZs) are host to anaerobic metabolisms that drive losses of bioavailable nitrogen from the ocean. The discovery of active nitrite-oxidising bacteria (NOB), long thought to be obligately aerobic, in AMZs has altered our perception of how nitrogen cycles in these oxygen-deficient waters. Yet, why NOB succeed in AMZs remains unclear. Here, we show that obligately aerobic NOB can thrive alongside aerobic microheterotrophs in AMZs via infrequent intrusions of oxygen. Ecological theory, biogeochemical modelling and metagenome-based maximum growth rate estimates suggest that NOB are opportunists that take advantage of periodic oxygen intrusions to rapidly accumulate biomass. Rather than harsh, AMZs prone to oxygen intrusions appear optimal for NOB, whose abundance and activity peaks in a 'goldilocks' zone of periodic oxygen and high nitrite supply. Our results recast the intermediate disturbance hypothesis to AMZs and highlight how the nitrogen cycle relies on dynamic coexistence of aerobic and anaerobic metabolisms.

Introduction

A deficit of nitrogen limits primary production across large areas of the ocean[1]. This widespread deficit originates from the anoxic marine zones (AMZs) that sit beneath the surface in the Eastern Pacific and Northern Indian Oceans. Consumption of oxygen in AMZs by respiring organisms generates a niche for anaerobic metabolisms, including denitrification ($NO_3^- \rightarrow NO_2^- \rightarrow NO \rightarrow N_2O \rightarrow N_2$) and anaerobic ammonium oxidation (anammox; $NH_4^+ + NO_2^- \rightarrow N_2$), both of which transform bioavailable nitrogen to elemental N_2 gas (Figure 1). Denitrification also produces nitrous oxide (N_2O), a potent greenhouse gas and ozone stripper[2]. As the ocean loses oxygen due to warming[3], nitrogen losses from denitrification and anammox may increase and intensify the nitrogen deficit across even larger swathes of the ocean[4].

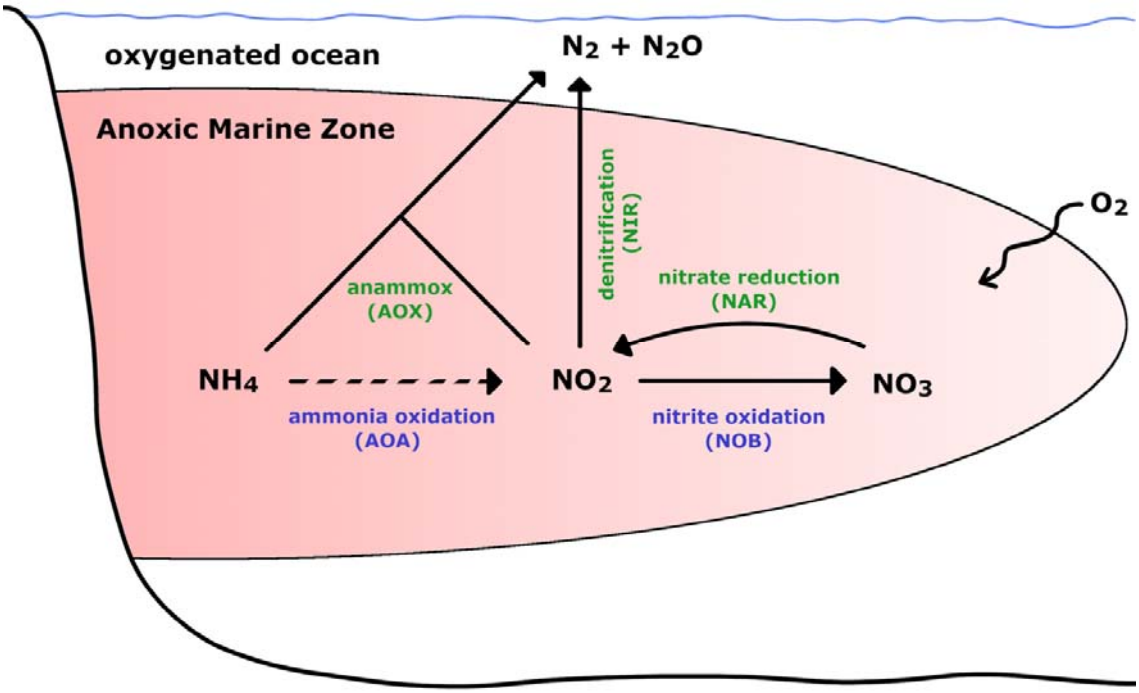

Figure 1. Nitrogen cycling in an anoxic marine zone (AMZ). Ammonium (NH_4^+) supplied by heterotrophic activity is either oxidised aerobically to nitrite (NO_2^-) by ammonia-oxidising archaea (AOA) or oxidised anaerobically in combination with NO_2^- to elemental dinitrogen gas (N_2) by anammox bacteria (AOX). Meanwhile, facultative heterotrophic bacteria perform denitrification when oxygen scarcity limits their growth. Denitrification (multi-step process from NO_3^- to N_2) occurs in two major steps. First, nitrate (NO_3^-) is reduced to NO_2^- by nitrate-reducing bacteria (NAR). Second, NO_2^- is reduced all the way to N_2 by nitrite-reducing bacteria (NIR), ignoring nitric oxide (NO) and nitrous oxide (N_2O) as intermediates. The NO_2^- that accumulates in AMZs (largely due to NAR) may then be oxidised back to NO_3^- by nitrite-oxidising bacteria (NOB). The broken arrow indicates slow rates of aerobic ammonia oxidation.

The relationship between deoxygenation and rates of nitrogen loss, however, is more complex. Once thought to be excluded from AMZs, aerobic ammonia oxidation ($NH_3 + O_2 \rightarrow NO_2^-$) and nitrite oxidation ($NO_2^- + O_2 \rightarrow NO_3^-$) that together form the two steps of

nitrification are now routinely observed[5–9]. Nitrite-oxidising bacteria (NOB) not only survive but thrive in AMZs (Figure 1), exhibiting some of the highest biomass and activity in anoxic waters[7,10–13]. The success of NOB in AMZs may alter rates of nitrogen loss and N_2O production, since denitrification and anammox may compete with NOB for nitrite when concentrations are low, but supply is high[14]. Such conditions are found at the edges of the AMZs at the anoxic-oxic interface. More fundamentally, the apparent success of aerobic NOB in AMZs challenges our conceptual understanding of the marine nitrogen cycle.

Multiple explanations for aerobic nitrification in AMZs have been proposed. High affinities for oxygen suggest that ammonia-oxidising archaea (AOA) and NOB can survive at nanomolar oxygen concentrations, which hints at a competitive edge against aerobic heterotrophs[14,15]. Meanwhile, there are suggestions that certain clades of NOB have evolved nitrite oxidation pathways using alternative electron acceptors[6,7], while AOA have developed means to support aerobic ammonia oxidation via anaerobic metabolisms that generate oxygen[16]. Others suggest that episodic oxygen supply to anoxic waters might be sufficient to sustain viable populations[9,15,17]. While these proposals are not mutually exclusive, any explanation would ideally also illuminate why AOA are in relatively low abundance and activity compared with thriving NOB[11,18].

Here, we identify the environmental and ecological conditions that allow for active aerobic nitrifiers in AMZs. We resolve the microbes that perform key nitrogen cycling metabolisms in a hierarchy of models to show that NOB can thrive in AMZs principally via infrequent oxygen intrusions. Metagenomic analysis suggests that NOB grow rapidly, enabling an opportunistic accumulation of biomass when they encounter the ‘goldilocks’ conditions of periodic oxygen and nitrite supply unique to AMZs, while AOA growth is slower and limited by ammonium supply. Our results show how a dynamic coexistence between aerobic and anaerobic metabolisms is a key feature of AMZs.

Stable anoxia does not allow aerobic nitrifiers

Previous theory and observations have demonstrated that aerobic and anaerobic metabolisms can coexist under stable anoxia[19–21]. This stable coexistence in principle applies to metabolisms competing for an electron donor (e.g., organic matter for heterotrophs), while aerobic metabolisms compete for oxygen. Because chemoautotrophic nitrification demands significantly more oxygen for growth than heterotrophic metabolisms, their oxygen subsistence concentration is higher, and so Zakem et al.[19] suggest that aerobic nitrifiers are outcompeted by aerobic heterotrophy when oxygen supply is low. In their model, only aerobic heterotrophs coexist with anaerobic metabolisms (denitrification and anammox) under stable anoxic conditions.

We updated the analysis by considering a broader array of traits of the major microbes inhabiting AMZs, including observations of cell size, carbon quota, stoichiometry, maximum growth rate, biomass yields and nutrient affinities (Supplementary Tables 1 and 2). In a virtual chemostat model with dynamic microbial populations (Figure 2a; methods), oxygen and organic matter were supplied at different ratios to generate an anoxic-oxic landscape (Figure 2b). In these stable conditions, as in Zakem et al.[19], AOA and NOB are competitively excluded from the anoxic regime by facultatively aerobic heterotrophs (Figure 2c). Despite

the high affinity of AOA and NOB for oxygen[9,14,15], which lowers the subsistence oxygen concentration required to support their growth into the nanomolar range (Supplementary Table 3), and widely varying traits of heterotrophs, heterotrophs appear to be superior competitors for oxygen (Supplementary Note 1; Supplementary Figure 1). We therefore cannot explain the coexistence of aerobic nitrifiers with anaerobic metabolisms in AMZs via a competitive upper hand for oxygen.

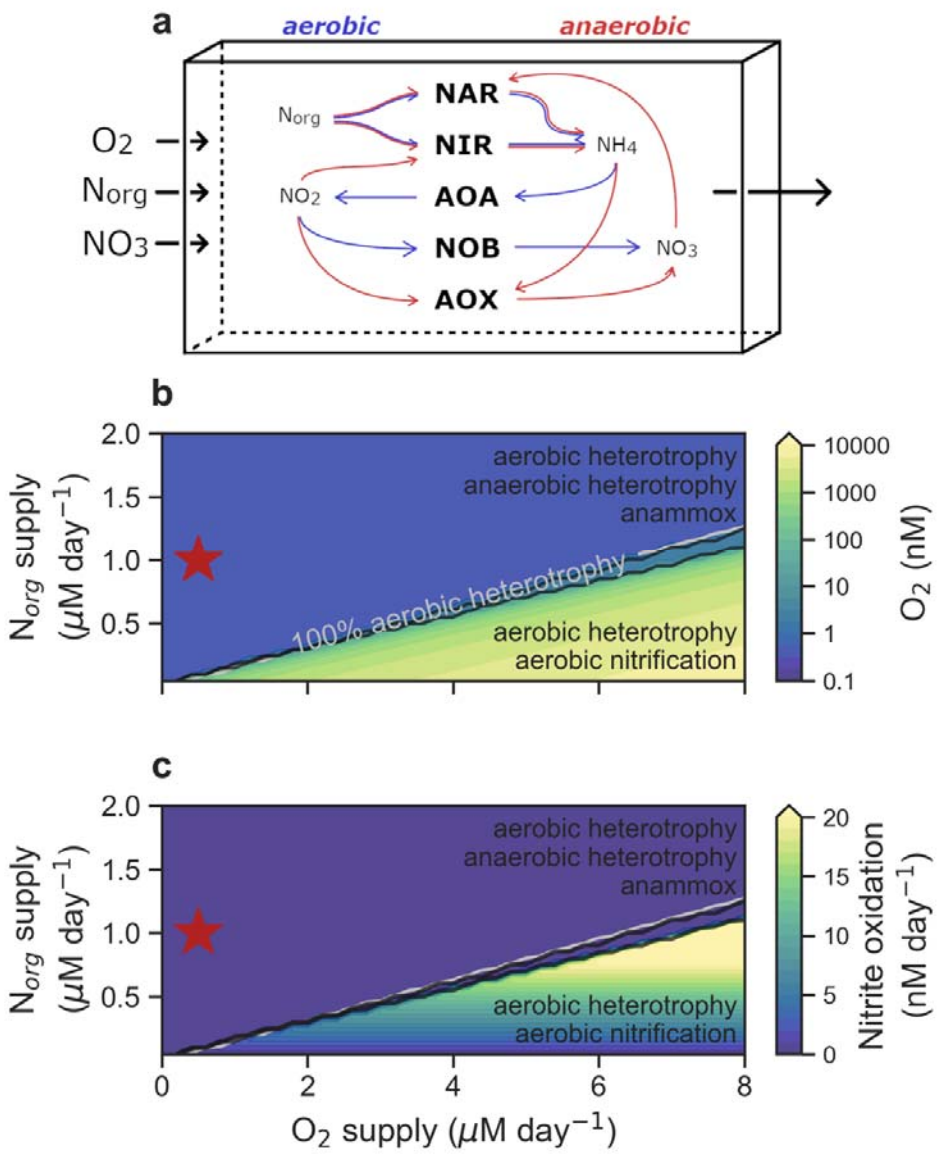

Figure 2. Steady-state outcomes of the chemostat model. a, Graphical representation of the chemostat experiments. The chemostat (single box model) contains aerobic (blue) and anaerobic (red) nitrogen cycling metabolisms carried about by key microbes: facultative nitrate- and nitrite- reducing heterotrophs (NAR and NIR), ammonia-oxidising archaea (AOA), nitrite-oxidising bacteria (NOB) and anammox bacteria (AOX). Nitrogen is

converted to elementary nitrogen (N_2) by NIR and AOX (not shown) and removed from the chemostat. **b**, Resulting steady-state oxygen concentration (nM) as a function of different rates of N_{org} and O_2 supply. **c**, Rate of nitrite oxidation (nM day^{-1}). The red star indicates the constant background N_{org} and O_2 supply rate used in the O_2 pulse experiments presented in Figure 4. Silver contour is the point below which 100 % of heterotrophy is aerobic. Black contours are the subsistence O_2 concentrations for AOA and NOB (Supplementary Table 3) indicating their competitive exclusion from the anoxic domain. Active metabolisms in the anoxic and oxic regimes are listed.

Aerobic nitrifiers viable with oxygen intrusions to AMZs

The prediction that facultatively aerobic heterotrophic microbes outcompete nitrifiers when oxygen is scarce is predicated on a stable environment[22]. However, AMZs are not stable. Time-varying intrusions of oxygen are evident from estimates of eddy-driven mixing[23], detection of nanomolar concentrations[24–26], and measurements of non-zero oxygen consumption rates in anoxic core waters[9,20].

Assuming (for now) that nitrifiers are obligately aerobic and neglecting limitation by micronutrients such as iron, we can consider oxygen intrusions to cause a population of nitrifiers to switch from oxygen-limited growth to nitrogen-limited growth (i.e., limitation by ammonium for AOA or nitrite for NOB) (Figure 3a). For the population to be sustained in its environment, growth must balance losses over time. Therefore, in a patchy environment with random intrusions of oxygen, the sum of oxygen-limited growth and nitrogen-limited growth must balance loss to predation, viral lysis, cell maintenance, and other mortality over a sufficiently long interval of time (methods). Following Litchman & Klausmier[27], we estimate the fraction of time, f, that nitrifiers must be released from oxygen-limited growth to sustain themselves in a low-oxygen environment (see derivation in the methods) as:

$$f = \frac{L - \mu_{O_2}}{\mu_N - \mu_{O_2}} \qquad 1$$

where μ_{O_2} and μ_N are the oxygen- and nitrogen-limited growth rates (day^{-1}), respectively, and L is the loss rate (day^{-1}).

Equation 1 can be further simplified if we make two assumptions. First, it may be reasonable for μ_{O_2} to be near-zero when oxygen is inaccessible due to consumption by heterotrophic bacteria, although this term may be greater than zero if we consider anaerobic metabolisms (see later). Second, if nitrite or ammonium accumulates then μ_N may approach the maximum growth rate (μ^{max}) of NOB or AOA, respectively. With both assumptions we find that

$$f \approx \frac{L}{\mu^{max}} \qquad 2$$

which suggests that the fraction of time that an aerobic nitrifier population must be released from oxygen limitation is approximated by the ratio of its loss rate to its maximum growth rate. If $L \ll \mu^{max}$, f approaches zero, meaning that nitrifiers may be viable in environments with infrequent oxygen intrusions.

In AMZs, it is typical for nitrite to accumulate and for ammonium to be depleted[7,17]. This difference in substrate availability provides a possible explanation for the different activities of NOB and AOA in AMZs. Growth on ammonium is not maximised for AOA ($\mu_N < \mu^{max}$), meaning they need more oxygen intrusions to sustain their biomass compared to NOB (Supplementary Figure 2). Limited availability of ammonium therefore makes AOA less viable in AMZs. In contrast, NOB may grow rapidly on nitrite once oxygen is non-limiting. Because Eqn. 2 suggests that a nitrifier is more viable with a higher maximum growth rate, we speculate that NOB may have an evolutionary incentive to optimise their maximum growth rate.

We have thus far supplied three predictions. One, trait-based analysis suggests that chemoautotrophic nitrifiers are intrinsically less competitive for oxygen than aerobic or facultatively aerobic heterotrophs (previous section). Two, theory shows that they can, however, survive in anoxia if there are infrequent oxygen intrusions. Three, the abundance of nitrite and scarcity of ammonium suggests that NOB are more viable than AOA in AMZs, and hints at an opportunistic life-strategy for NOB[27]. We next tested these theoretical predictions in the numerical model.

Simulations support theory

We applied abrupt pulses of oxygen to the chemostat model (Figure 2a) at varying amplitudes and frequencies. Pulse amplitudes of up to 1 µM are consistent with measured rates of oxygen consumption under anoxic conditions[20]. Pulse periods of < 1 to 10 days are consistent with known mechanisms of oxygenation, including high frequency turbulent mixing, diurnal cycles of oxygenic photosynthesis[21], and lower-frequency (i.e., weekly) eddy activity[23]. We applied these pulses on top of a constant oxygen supply of 0.5 µM day^{-1} and organic matter supply of 1 µM day^{-1}, which were conditions that generated deep anoxia and excluded nitrifiers under steady-state (red star in Figure 2b,c).

As predicted, the episodic pulses sustained a population of NOB in anoxic conditions. Most pulse experiments (run over 10,000 model days) became essentially anoxic, containing less than 25 nM of oxygen (averaged over final 100 days; Figure 3b). Even large oxygen pulses were rapidly drawn down by the microbial community, which quickly returned the system to anoxia. Mean nitrite oxidation rates were substantially larger with oxygen pulses than at steady state, reaching values as high as 500 nM day^{-1} (Figure 3c). Thus, NOB coexisted with anammox bacteria and denitrifying heterotrophs. In fact, active nitrite oxidation (> 1 nM day^{-1}) was present in the majority (80 %) of the experiments with active anaerobic metabolisms and was only excluded under the most oxygen-deprived conditions, perhaps analogous to an AMZ core where intrusions are rare[28]. Meanwhile, aerobic AOA was not sustained despite oxygen pulses because of competition with anammox bacteria for a scarce ammonium supply (Supplementary Figure 3).

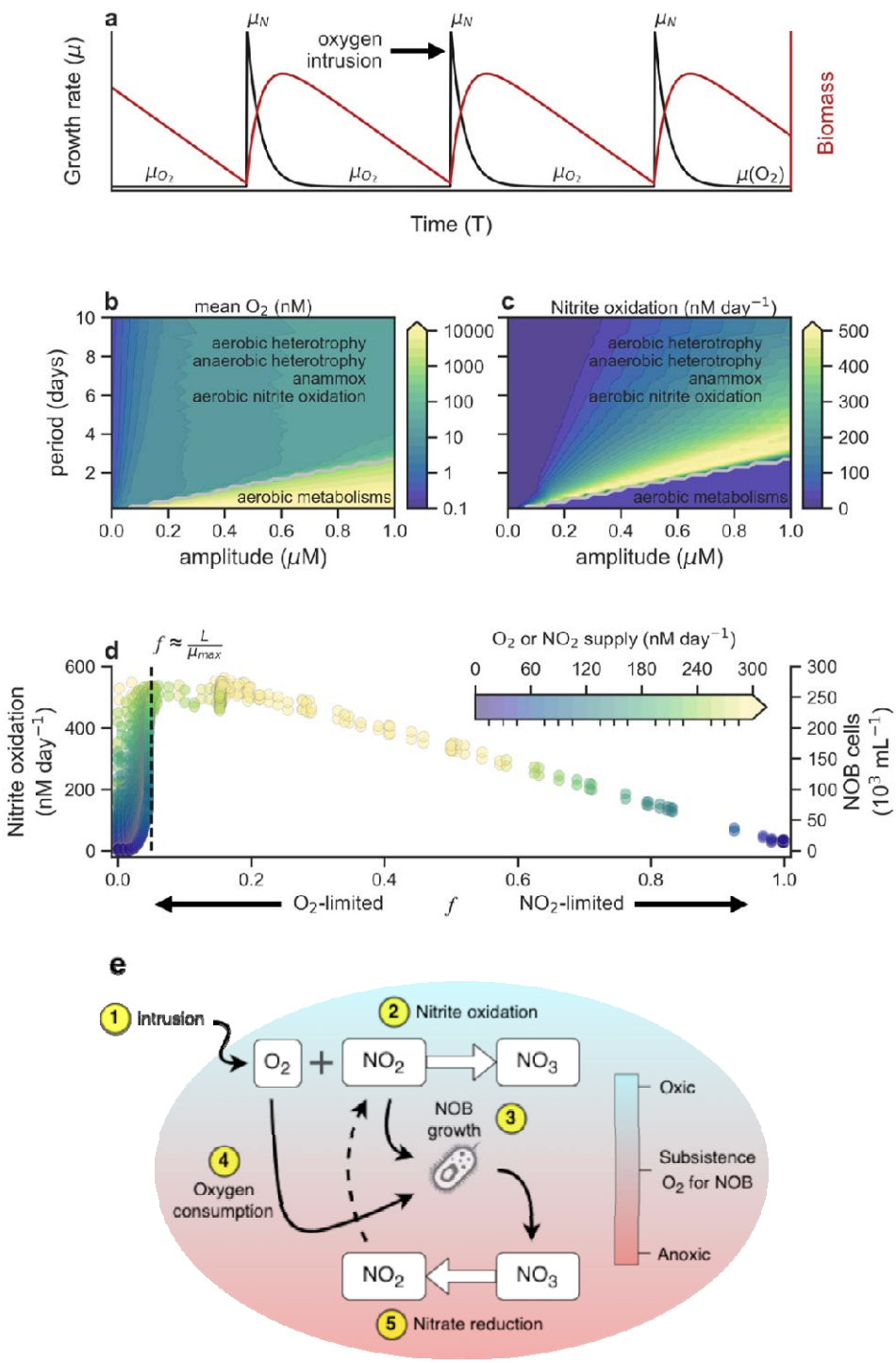

Figure 3. Episodic oxygen pulses support nitrite oxidation. a, Graphical representation of oxygen intrusions to an anoxic water parcel causing a shift from an oxygen-limited growth rate ( ) to a nitrogen-limited growth rate ( ), which causes distinct periods of biomass accumulation followed by loss after a return to (red). **b**, Average concentration of dissolved oxygen (O_2) in nanomolar (nM) over last 100 days of chemostat experiments (run to equilibrium) with background oxygen and organic matter supply of 0.5 and 1.0 μM day^{-1}

(red star in Figure 2b,c). Silver line represents threshold where 100 % of heterotrophy becomes aerobic. Active metabolisms in the anoxic and oxic regimes are listed. **c**, Average rate of nitrite oxidation in nM day^{-1}. **d**, Relationship between f, the rate of nitrite oxidation (left y-axis) and NOB abundance (left y-axis; assumes NOB contain 39.8 fg C per cell[29]. Points are coloured by the average rate of oxygen or nitrite supply, whichever is lowest (nM day^{-1}). The dotted line in panel **d** represents the analytically derived f value for NOB in AMZs (Eqn. 2). **e**, The stabilising biological feedback of NOB in response to oxygen intrusions, whereby (1) greater intrusions stimulate (2) nitrite oxidation, leading to (3) gains in NOB biomass, which in turn elevates (4) oxygen consumption and a more rapid return to anoxia, thereby generating nitrite via (5) nitrate reduction.

AMZs as optimal environments for NOB

Interestingly, the activity and biomass of aerobic NOB increased with the strength and frequency of oxygen pulses, but only if the system returned to anoxia. A return to anoxia allowed for high rates of heterotrophic nitrate reduction to nitrite (Figure 1). This pathway for nitrite supply, unavailable in oxygenated conditions, was key to maximising NOB biomass and activity (Figure 3d).

It follows that oxygen consumption by NOB represents a biological feedback to oxygen intrusions that both stabilises the environment (i.e., maintains anoxia) and ensures nitrite supply (Figure 3e). NOB are observed to contribute substantially to oxygen consumption in low-oxygen settings[9], and in our experiments obligately aerobic NOB flourished when they contributed substantially to total oxygen consumption (Supplementary Figure 4). This feedback was evident from how modelled f (the proportion of time oxygen was not limiting to NOB growth) approximated our analytically derived value of $f = \frac{L}{\mu^{max}}$ (Eqn. 2). 50 % of experiments resulted in f values within 2 % (± 0.02) of $\frac{L}{\mu^{max}}$ (Figure 3d; Supplementary Figure 5). If no biological feedback existed, f would increase proportionally with the intensity of oxygen pulsing. Instead, as oxygen pulsing intensified and supported more nitrite oxidation, the biomass of NOB grew and consumed more oxygen, thus more rapidly returning the system to anoxia and stimulating nitrate reduction to resupply nitrite (Figure 3e).

Far from being harsh environments, AMZs prone to oxygen intrusions appear favourable for aerobic NOB. Since heterotrophic nitrate reduction scales with organic matter supply[30], nitrite supply is most likely maximised at the top of AMZs where organic matter flux is greatest and where NOB biomass and activity are observed to peak[5–8,31]. At these locations, NOB biomass, sustained by infrequent oxygen intrusions, could also access diurnal oxygen supply from phytoplankton growing in the anoxic secondary chlorophyll maximum[21]. The importance of supply as demonstrated here also explains why *in situ* concentrations of oxygen and nitrite have little skill for predicting nitrite oxidation rates[12,15,32,33].

Gene-based maximum growth rates support theory

Our theory suggests that rapid growth following oxygen intrusions is key to NOB success in AMZs. This leads to a hypothesis that the novel clades of NOB that inhabit AMZs[14,31] have

adapted to an opportunistic lifestyle by optimising their potential for rapid growth. This potential may emerge in these clades' maximum growth rates[27], . Faster would allow obligately aerobic NOB clades to sustain themselves with less frequent oxygen intrusions (Eqn. 2), potentially facilitating the colonisation of AMZ core waters where intrusions are rarer[28].

To test this hypothesis, we estimated from metagenome-assembled genomes[34] of NOB (*Nitrospinae spp.*), AOA (*Nitrosopumilus spp.* and *Nitrosopelagicus spp.*), and heterotrophic bacteria (*Pelagibacter spp.*) collected from the Eastern Tropical South Pacific AMZ[10]. of NOB (1.7 – 1.8 day^{-1}) were higher than those of AOA (0.9 – 1.3 day^{-1}), which in turn were higher than those of *Pelagibacter spp.* (0.5 – 0.8 day^{-1}) (Figure 4). NOB metagenome-assembled genomes were also classified as copiotrophs according to defined codon-usage bias thresholds[34], while AOA and *Pelagibacter spp.* were classified as oligotrophs. The higher of NOB inhabiting AMZs and their classification as copiotrophs suggests that NOB can be considered opportunists, primed to take advantage of oxygen intrusions relative to the other dominant oxygen-consuming microbial types.

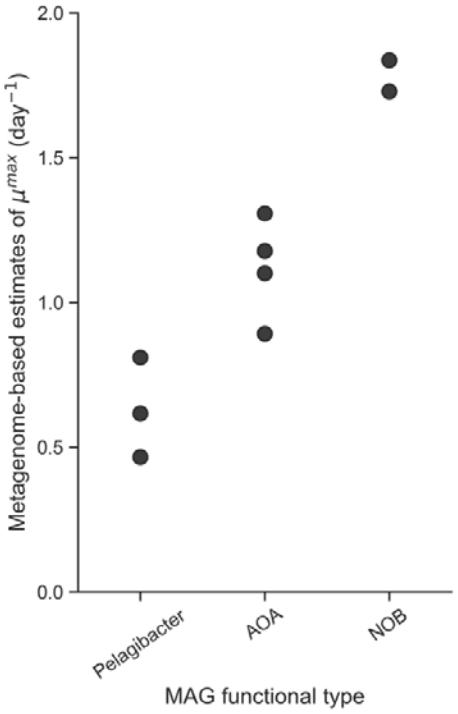

Figure 4. Metagenome-based estimates of maximum growth rates of key microbes inhabiting AMZs. Estimates are from metagenome-assembled genomes (MAGs) from the East Tropical South Pacific oxygen minimum zone[10] using codon usage patterns[34].

Illustrations from an ocean-biogeochemical model

To test aerobic NOB sustainability in AMZs in a more realistic environment, we encoded diverse oxygen- and nitrogen-cycling heterotrophic and chemoautotrophic microbial populations into an ocean-biogeochemical model and performed one-dimensional simulations (water column) based in the offshore Southeast Pacific. Oxygen was introduced throughout the water column once per week to emulate lateral supply via passing eddy filaments[23]. The model produced an AMZ between 200 and 700 metres when there was no lateral oxygen supply, and steadily shrunk in vertical extent with increasing oxygen supply until it disappeared under the strongest oxygen pulses (Figure 5a). Shrinking of the AMZ was associated with decreases in nitrite from a maximum of 8.5 µM to less than 0.01 µM when no AMZ was present (Figure 5b).

The activity and biomass of NOB increased with the strength of oxygen intrusions (Figure 5c,d). With no intrusions, nitrite oxidation peaked at ~30 nM day^{-1} in the upper AMZ and showed a secondary peak at the bottom of the AMZ. These local peaks in NOB activity and biomass at the edges of the AMZ were associated with the transition between regimes of high oxygen and nitrite supply. In the AMZ core, however, nitrite oxidation was negligible (< 0.1 nM day^{-1}). Oxygen intrusions elevated rates by orders of magnitude. Maximum rates of ~350 nM day^{-1} developed at the top of the AMZ, while rates of roughly 100 nM day^{-1} developed in the anoxic core. These simulated rates approximated those measured in the ocean (Figure 5c), although were not high enough to match some very high rates (> 500 nM day^{-1}) from one station in the southeast Pacific[12]. These high rates were, however, simulated in our chemostat experiments (Figure 3c) and may represent high organic matter supply at the time of sampling.

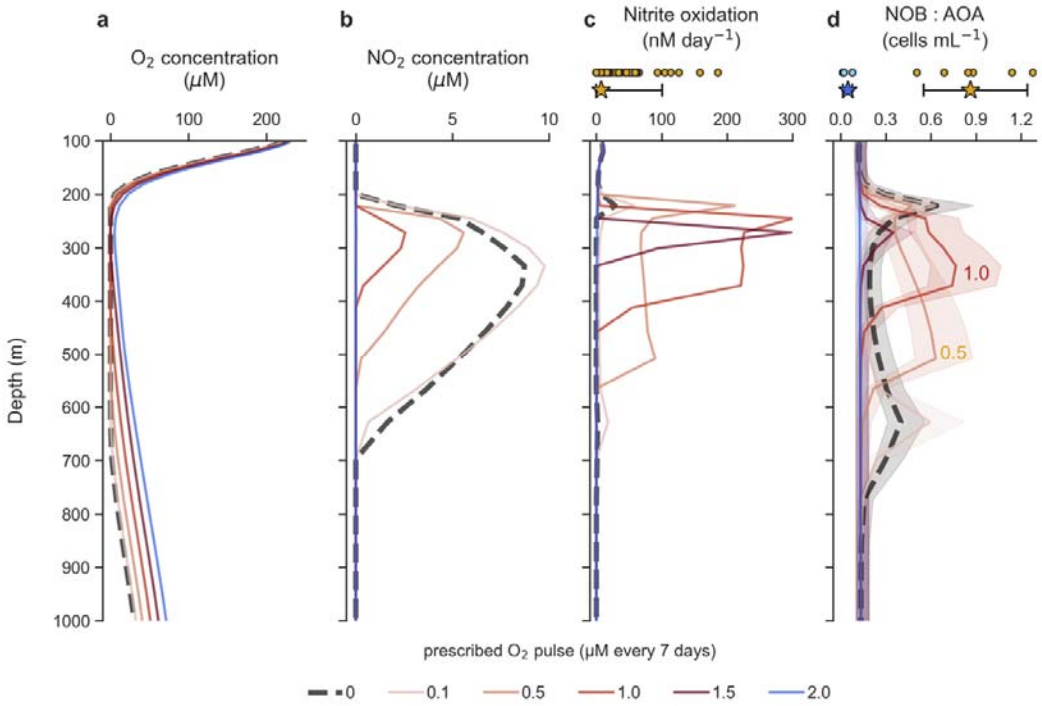

Figure 5. Oxygen pulsing supports nitrite oxidation in a one-dimensional water column model. a, Average concentration of dissolved oxygen (O_2; µM). **b**, Average concentration of nitrite (NO_2; µM). **c**, Maximum rate of nitrite oxidation (nM day^{-1}). Observed nitrite

oxidation rates within low-oxygen waters (gold circles) in locations across the East Pacific[7,12] are shown above. **d**, Ratio of nitrite-oxidising bacteria (NOB) to ammonia-oxidising archaea (AOA) in cells per mL. Biomass as output by the model is converted to cells per mL assuming 39.8 fg carbon per cell of NOB and 11.5 fg carbon per cell of AOA, with shading indicating a range of NOB carbon content from 26.8 to 51 fg per cell (methods)[29]. Observed NOB:AOA in the data above panel **d** are counts of genes encoding nitrite oxidoreductase (Nxr) to ammonia monooxygenase (amoA)[13], assuming that there are 4 copies of Nxr per NOB cell. Blue data are from oxygenated waters. Gold data are from the AMZ. The star and error bars show the median and 5th to 95th percentile spread of the observations.

Meanwhile, ammonia oxidation did not respond similarly to oxygen intrusions, showing a weak peak near the top of the AMZ and rates lower than 5 nM day^{-1} though the core (Supplementary Figure 6), consistent with observations[9,12]. The abundance of NOB relative to AOA therefore peaked in the AMZ and was amplified by oxygen intrusions (Figure 5d). Based on the ratio of concentrations of key genes that encode the main enzymes involved in nitrite oxidation (Nxr) and ammonia oxidation (amoA), Fuchsman et al.[13] identified a significant increase in the relative abundance of NOB within the oxygen deficient zone of the eastern North Pacific. Our simulated increase in NOB to AOA abundance, converted from modelled biomass using a range of carbon quotas for AOA and NOB grown in environmental relevant conditions [29] (see methods), is consistent with the observed increase in NOB to AOA in oxygen deficient zones (gold markers) compared to oxygenated waters (blue markers).

Implications for the ecology and nitrogen cycle of AMZs

Our results indicate that NOB may be adapted to take advantage of a 'goldilocks zone' of episodic oxygenation and high nitrite supply in AMZs. AOA, in contrast, are limited by competition with anammox bacteria for a weak supply of ammonium, which explains the difference in observed activities of these microbes in AMZs. Novel clades of NOB that inhabit AMZs[10,31] appear well-suited for the AMZ environment. High maximum growth rates compared with other microbes in AMZs (Figure 5; Supplementary Table 1) indicate that NOB have adapted towards an opportunist lifestyle, characterised by a propensity for relatively fast growth[27]. As opportunists, NOB can bloom during resource pulses to an extent that offsets losses of biomass during resource scarcity.

The observed peak in NOB activity and biomass in AMZs is herein explained by obligately aerobic metabolism. Growth via alternative electron acceptors[6,7] would be complementary, but not necessary, where oxygen intrusions occur. Facultatively anaerobic growth would, however, increase aerobic NOB viability. If anaerobic growth is possible, then μ_{O_2} in Eqn. 1 becomes positive, making nitrifiers even less reliant on oxygen intrusions (Supplementary Figure 7). NOB may also reverse the nitrite oxidoreductase enzyme and perform heterotrophic nitrate reduction[33,35], which would further consolidate AMZs as optimal environments for NOB because nitrate reduction during anaerobic growth would supply the very nitrite required for aerobic growth (Figure 3e).

Our picture of how NOB survive in AMZs is consistent with the intermediate disturbance hypothesis of ecology[36]. Oxygen intrusions in AMZs (Figure 1) are analogous to storm events

on coral reefs, clearance events in rain forests, or mixing events in the sunlit surface ocean that disturb the ecosystem and increase diversity[36,37]. Intrusions periodically switch the competitive upper hand by shifting limiting resources, which accelerates trait differentiation and drives speciation along an opportunist-gleaner spectrum[27,38]. Microbial ecology in AMZs may therefore offer fertile ground for testing ecological theories linking disturbance, coexistence, and trait differentiation.

We propose that the success of NOB in AMZs is contingent on a time-varying circulation of the ocean not typically included in the coarse resolution models currently used for climate change impact assessments[3]. Mixing due to eddies and turbulence is therefore not only key for resolving the state and evolution of the oxygen concentrations defining AMZs themselves[39,40], but also for resolving the microbial communities that inhabit AMZs and that drive critical nitrogen transformations. NOB are particularly important in this regard. By competing with the major anaerobic metabolisms for nitrite, NOB can alter N_2O production and losses of bioavailable nitrogen from an already nitrogen-limited ocean[1]. Higher resolution Earth System Models that resolve (sub)mesoscale mixing processes would account for the dynamic coexistence of heterotrophic and chemoautotrophic microbes and likely generate more accurate projections of the biogeochemical consequences of expanding AMZs.

Methods

Derivation of f

The growth rate μ (day^{-1}) of a given nitrifier population can be expressed as a function of the limitation to growth by either nitrogen (μ_N) or oxygen (μ_{O_2}), assuming Liebig's law of the minimum, as:

$$\mu = \min(\mu_N, \mu_{O_2}) \qquad 3$$

When neglecting the impacts of physical transport, the biomass (B; mol N m^{-3}) of the population changes according to μ and its loss rate L (day^{-1}), which reflects the impacts of viral lysis, grazing, and other mortality, as:

$$\frac{\partial B}{\partial t} = (\mu - L)B \qquad 4$$

For the population to be sustained in its environment, growth must balance losses. In a time-varying environment, this balance can be found over a sufficiently long interval of time (I) so that the integrated growth balances the integrated losses over time as:

$$\int_I \mu \, dt = \int_I L \, dt \qquad 5$$

In a patchy environment with random intrusions of oxygen there may be multiple phases of growth controlled by oxygen limitation interspersed by growth controlled by nitrogen limitation (Figure 3a). Following Litchman & Klausmier[27], we can decompose the integrated growth rate into two aggregate sub-intervals, one interval of N limitation I_N and one interval of O_2 limitation I_{O_2}, which need not be continuous in time, as:

$$\int_{I_N} \mu_N \, dt + \int_{I_{O_2}} \mu_{O_2} \, dt = \int_I L \, dt \qquad 6$$

Then we define f as the fraction of time during interval I where nitrifiers are limited by nitrogen (i.e., released from oxygen limitation), and $(1 - f)$ is the fraction of time where they are limited by oxygen. Neglecting any time dependence of loss rates and integrating over time gives

$$f\mu_N + (1 - f)\mu_{O_2} = L \qquad 7$$

Solving for f gives the fraction of time that the nitrifying population can be released from limitation by oxygen to sustain itself in the environment:

$$f = \frac{L - \mu_{O_2}}{\mu_N - \mu_{O_2}} \qquad 8$$

Zero-dimensional chemostat model

We use a zero-dimensional, theoretical model resolving multiple microbial functional type populations carrying out distinct nitrogen-cycling metabolisms[19]. The metabolic functional

types include two types of facultative heterotrophs that use oxygen for aerobic heterotrophy and either nitrate (NAR) or nitrite (NIR) as electron acceptors, anaerobic ammonium oxidation by anammox bacteria (AOX), aerobic ammonia oxidation by ammonia-oxidising archaea (AOA), and aerobic nitrite oxidation by nitrite-oxidising bacteria (NOB). Each metabolism requires two resources, an electron donor (S) and an electron acceptor (X), and each is performed by a microbe with unique traits (Supplementary Table 1). These traits govern the competitive ability of the microbe for the resources on which they depend and the rate at which their biomass accumulates.

The basic economy of the model is in nitrogen, such that biomass is resolved in units of mol N_{bio} m^{-3}. Growth is the product of the specific uptake rate of a resource (V, mol resource (mol N_{bio})$^{-1}$ day^{-1}) multiplied by the biomass yield associated with that resource (y, mol N_{bio} (mol resource)$^{-1}$). The realised growth rate (μ, day^{-1}) is the minimum of growth on S or X.

$$\mu = \min\,[V_S y_S, V_X y_X] \qquad 9$$

The specific uptake of a resource (V_S, V_X), except oxygen, is calculated via michaelis-menten kinetics using a maximum specific uptake rate (V_S^{max}, V_X^{max}) and a half-saturation coefficient (K_S, K_X).

$$V_S = V_S^{max}\frac{S}{S + K_S} \qquad 10$$

$$V_X = V_X^{max}\frac{X}{X + K_X} \qquad 11$$

For dissolved oxygen, we assume that the specific uptake rate (V_{O_2}) is limited by diffusive supply [22], which is dependent on the radius of the cell (r, metres), the diffusion coefficient of oxygen in seawater (D, m^2 day^{-1}), the cellular quota of nitrogen (Q_N, mol N_{bio} μm^{-3}) multiplied by the volume of the cell (μm^3), and the ambient oxygen concentration (O_2, mol m^{-3}).

$$V_{O_2} = \frac{4\pi r D}{Q_N V} O_2 \qquad 12$$

The radius of the cell is calculated from the cellular volume (Supplementary Table 1), the diffusion coefficient is $1.5613 \cdot 10^{-5}$ cm^2 s^{-1} corresponding to 12 °C and 35 psu (https://unisense.com/wp-content/uploads/2021/10/Seawater-Gases-table.pdf), and the cellular quota of nitrogen is solved for using estimates of carbon quotas and cell volume.

State variables are organic matter (OM), inorganic nutrients (NH_4^+, NO_2^-, NO_3^-), dissolved dinitrogen (N_2), dissolved oxygen (O_2) and the biomass of each microbial group (B_{NAR}, B_{NIR}, B_{AOA}, B_{NOB}, B_{AOX}). Complete equations for each state variable in the chemostat are as follows:

$$\frac{dOM}{dt} = -\left(\frac{\mu_{NAR} B_{NAR}}{y_{NAR}^{OM}}\right) - \left(\frac{\mu_{NIR} B_{NIR}}{y_{NIR}^{OM}}\right) + dil(OM_{in} - OM) \qquad 13$$

$$\frac{dO_2}{dt} = -\left(\frac{\mu_{NAR}B_{NAR}}{y_{NAR}^{O_2}}\varphi_{NAR}\right) - \left(\frac{\mu_{NIR}B_{NIR}}{y_{NIR}^{O_2}}\varphi_{NIR}\right) - \left(\frac{\mu_{AOA}B_{AOA}}{y_{AOA}^{O_2}}\right) - \left(\frac{\mu_{NOB}B_{NOB}}{y_{NOB}^{O_2}}\right) + dil\left(O_{2,in} - O_2\right) \quad 14$$

$$\frac{dNH_4^+}{dt} = -\left(\frac{\mu_{AOA}B_{AOA}}{y_{AOA}^{NH_4^+}}\right) - \left(\frac{\mu_{AOX}B_{AOX}}{y_{AOX}^{NH_4^+}}\right) - (\mu_{NOB}B_{NOB}) + \left(\mu_{NAR}B_{NAR}\left(\frac{1}{y_{NAR}^{OM}} - 1\right)\right) + \left(\mu_{NIR}B_{NIR}\left(\frac{1}{y_{NIR}^{OM}} - 1\right)\right) + dil\left(NH_{4,in}^+ - NH_4^+\right) \quad 15$$

$$\frac{dNO_2^-}{dt} = -\left(\frac{\mu_{NIR}B_{NIR}}{y_{NIR}^{NO_2^-}}(1-\varphi_{NIR})\right) - \left(\frac{\mu_{NOB}B_{NOB}}{y_{NOB}^{NO_2^-}}\right) - \left(\frac{\mu_{AOX}B_{AOX}}{y_{AOX}^{NO_2^-}}\right) + \left(\mu_{AOA}B_{AOA}\left(\frac{1}{y_{AOA}^{NH_4^+}} - 1\right)\right) + \left(\frac{\mu_{NAR}B_{NAR}}{y_{NAR}^{NO_3^-}}(1-\varphi_{NAR})\right) + dil\left(NO_{2,in}^- - NO_2^-\right) \quad 16$$

$$\frac{dNO_3^-}{dt} = -\left(\frac{\mu_{NAR}B_{NAR}}{y_{NAR}^{NO_3^-}}(1-\varphi_{NAR})\right) + \left(\frac{\mu_{NOB}B_{NOB}}{y_{NOB}^{NO_2^-}}\right) + \left(\mu_{AOX}B_{AOX}e_{AOX}^{NO_3^-}\right) + dil\left(NO_{3,in}^- - NO_3^-\right) \quad 17$$

18

$$\frac{dN_2}{dt} = \left(\frac{\mu_{NIR}B_{NIR}}{y_{NIR}^{NO_2^-}}(1-\varphi_{NAR})\right) + \left(\mu_{AOX}B_{AOX}e_{AOX}^{N_2}\right) + dil(-N_2) \quad 19$$

$$\frac{dB_{NAR}}{dt} = (\mu_{NAR}B_{NAR}) + dil(-B_{NAR}) + \alpha(B_{NAR})^2 \quad 20$$

$$\frac{dB_{NIR}}{dt} = (\mu_{NIR}B_{NIR}) + dil(-B_{NIR}) + \alpha(B_{NIR})^2 \quad 21$$

$$\frac{dB_{AOA}}{dt} = (\mu_{AOA}B_{AOA}) + dil(-B_{AOA}) + \alpha(B_{AOA})^2 \quad 22$$

$$\frac{dB_{NOB}}{dt} = (\mu_{NOB}B_{NOB}) + dil(-B_{NOB}) + \alpha(B_{NOB})^2 \quad 23$$

$$\frac{dB_{AOX}}{dt} = (\mu_{AOX}B_{AOX}) + dil(-B_{AOX}) + \alpha(B_{AOX})^2 \quad 24$$

The dilution rate (dil) in day^{-1} is set as a constant, while the mortality of biomass may be made a quadratic function of biomass in a 'kill-the-winner' approach by making α positive. We also control aerobic versus anaerobic growth via a Heaviside function stored in φ_{NAR} and φ_{NIR} for facultative heterotrophs.

$$\varphi = \begin{cases} 0, & if\ \mu^{NO_X^-} > \mu^{O_2} \\ 1, & if\ \mu^{O_2} > \mu^{NO_X^-} \end{cases} \quad 25$$

The default values of the yields of each metabolism are listed in Supplementary Table 2.

Competitive outcomes of chemostat model

The competitive outcomes of the chemostat model can be anticipated by solving for the population-specific resource subsistence concentrations, R*[41], by assuming steady-state such that growth (μ) equals losses (L) of biomass. For organic matter and inorganic nutrients, the R* is calculated for resource i and population j as:

$$R_{ij}^{*} = \frac{K_{ij} L_j}{y_{ij} V_{\mathrm{ij}}^{\max} - L_j} \qquad 26$$

For dissolved oxygen, O_2*, we use the equation derived in Zakem & Follows[22] for population j:

$$O_2^{*} = \frac{L_j Q_{C,j} r_j^2}{3 D y_{O_2,j}} \qquad 27$$

Where the carbon quota of the cell (Q_C), radius (r), diffusion coefficient (D) and yield (y^{O_2}) are in units of mol C μm^{-3}, μm, μm^2 day^{-1} and mol C_{bio} (mol O_2)$^{-1}$, respectively. This equation will return similar values to an R* derived from Michaelis-Menton kinetics (Eqn. 26) when considering very high affinities (very low $\frac{K_{ij}}{V_{\mathrm{ij}}^{\max}}$).

Estimating maximum growth rate from draft metagenomes

Metagenome-assembled genomes (MAGs) were generated from water samples taken in the anoxic zone in the Eastern Tropical South Pacific Ocean[10]. We annotated each MAG using *prokka*[42] (with options --norrna --notrna --centre X --compliant and --kingdom Archaea when dealing with archaeal MAGs) to obtain coding sequences and locate ribosomal proteins. We then performed growth prediction as a function of codon usage bias of the ribosomal proteins with gRodon[34] assuming an optimal growth temperature of 13 °C for all MAGs based on the mean of sample temperatures and using metagenome mode v2[43] to control for any possible contamination caused by binning. Weissman et al.[43] provide a cut-off to classify an organism as a copiotroph or oligotroph (i.e., opportunists or gleaners[27]). The cut off is based on where the codon usage bias versus minimum doubling time curve saturates[34].

One-dimensional water column model

The biogeochemical model is the Pelagic Interactions Scheme for Carbon and Ecosystem Studies version 2 (PISCES-v2), which is attached to the Nucleus for European Modelling of the Ocean version 4.0 (NEMO-v4) general ocean circulation model. PISCES-v2 already explicitly simulates the biomass of two phytoplankton and two zooplankton types[44]. Biomass pools of facultative nitrate- and nitrite-reducing heterotrophs, anammox bacteria, ammonia-oxidising archaea and nitrite-oxidising bacteria were added to PISCES-v2 with the same traits and yields as in the chemostat model (Supplementary Tables 1 and 2). Nitrite was also added as a tracer with sources of ammonia oxidation and denitrification, and sinks of denitrification, nitrite oxidation, anammox and phytoplankton assimilation.

Three-hourly atmospheric conditions to force the model were taken from the JRA55-do atmospheric reanalysis product at 10°S, 82°W at year 2010[45]. The model was initialised at this location with temperature, salinity, oxygen, phosphate, nitrate, and silicate from the World Ocean Atlas[46–49], dissolved inorganic carbon and alkalinity from the Global Ocean Data Analysis Project version 2 (GLODAPv2)[50], and iron and dissolved organic carbon from a previous global solution of NEMO-PISCES-v2. Ammonium and nitrite were initialised at 0 mmol m^{-3}, and all biomasses were initialised at 0.01 mmol C m^{-3}.

Each simulation was run for 11 years, and all results are presented as water column averages over the final year. The first year of each simulation was conducted with no oxygen pulses. Oxygen pulses of varying magnitudes were then applied over the subsequent 10 years. Pulses of 0.0, 0.1, 0.5, 1.0, 1.5, and 2.0 µM were applied every 7 days, emulating the possible effect of passing eddy filaments to an AMZ.

We present in Supplementary Figure 8 key variables of temperature, salinity, mixed-layer depth, oxygen, nitrite, nitrate, and microbial biomasses in a simulation run out to 100 years. This shows an initial intensification of the AMZ in the first decade, followed by the downward migration and gradual degradation of the AMZ by year 25. Depth integrals of microbial biomass show arrival at quasi-equilibrium by year 10 and a temporal maximum in nitrite concentration within the AMZ. Year 11 therefore represented a quasi-equilibrium in microbial biomasses and a distinct AMZ. We conducted a suite of sensitivity experiments to ensure that model output did not qualitatively differ with different initial concentrations of microbial biomasses, which were varied by over 100-fold from 0.001 to 0.1 mmol C m^{-3} (Supplementary Figure 9).

Carbon quotas and yields for AOA and NOB

As in Zakem et al.[51], we convert modelled biomass to cell abundances using measured carbon quotas for AOA and NOB grown in natural seawater at 15°C and 1 µM substrate[29]. For AOA, we use the average carbon content from *Ca. Nitrosopelagicus* U25 and *Nitrosopumilus* sp. CCS1: 11.5 ± 2.0 fgC per cell. For NOB, we use the carbon content of *Nitrospina* sp. Nb-3: 39.8 ± 11.2 fg C per cell. We also use the measured carbon fixation yields from these organisms as the biomass yields for AOA and NOB in our model (Supplementary Table 1).

References

1. Moore, C. M. Diagnosing oceanic nutrient deficiency. *Philosophical Transactions of the Royal Society A: Mathematical, Physical and Engineering Sciences* **374**, 20150290 (2016).

2. Ravishankara, A. R., Daniel, J. S. & Portmann, R. W. Nitrous Oxide (N2O): The Dominant Ozone-Depleting Substance Emitted in the 21st Century. *Science (1979)* **326**, 123–125 (2009).

3. Bindoff, N. L. *et al.* Changing Ocean, Marine Ecosystems, and Dependent Communities. in *IPCC Special Report on the Ocean and Cryosphere in a Changing Climate* (eds. Portner, H.-O. et al.) 447–588 (2019). doi:https://www.ipcc.ch/report/srocc/.

4. Canfield, D. E., Glazer, A. N. & Falkowski, P. G. The evolution and future of earth's nitrogen cycle. *Science (1979)* **330**, 192–196 (2010).

5. Füssel, J. *et al.* Nitrite oxidation in the Namibian oxygen minimum zone. *ISME J* **6**, 1200–1209 (2012).

6. Babbin, A. R. *et al.* Multiple metabolisms constrain the anaerobic nitrite budget in the Eastern Tropical South Pacific. *Global Biogeochem Cycles* **31**, 258–271 (2017).

7. Babbin, A. R., Buchwald, C., Morel, F. M. M., Wankel, S. D. & Ward, B. B. Nitrite oxidation exceeds reduction and fixed nitrogen loss in anoxic Pacific waters. *Mar Chem* **224**, 103814 (2020).

8. Beman, J. M., Leilei Shih, J. & Popp, B. N. Nitrite oxidation in the upper water column and oxygen minimum zone of the eastern tropical North Pacific Ocean. *ISME J* **7**, 2192–2205 (2013).

9. Beman, J. M. *et al.* Substantial oxygen consumption by aerobic nitrite oxidation in oceanic oxygen minimum zones. *Nat Commun* **12**, 7043 (2021).

10. Sun, X. & Ward, B. B. Novel metagenome-assembled genomes involved in the nitrogen cycle from a Pacific oxygen minimum zone. *ISME Communications* **1**, 26 (2021).

11. Peng, X. *et al.* Ammonia and nitrite oxidation in the Eastern Tropical North Pacific. *Global Biogeochem Cycles* **29**, 2034–2049 (2015).

12. Santoro, A. E. *et al.* Nitrification and Nitrous Oxide Production in the Offshore Waters of the Eastern Tropical South Pacific. *Global Biogeochem Cycles* **35**, 1–21 (2021).

13. Fuchsman, C. A., Devol, A. H., Saunders, J. K., McKay, C. & Rocap, G. Niche partitioning of the N cycling microbial community of an offshore oxygen deficient zone. *Front Microbiol* **8**, 1–18 (2017).

14. Sun, X., Frey, C., Garcia-Robledo, E., Jayakumar, A. & Ward, B. B. Microbial niche differentiation explains nitrite oxidation in marine oxygen minimum zones. *ISME J* **15**, 1317–1329 (2021).

15. Bristow, L. A. *et al.* Ammonium and nitrite oxidation at nanomolar oxygen concentrations in oxygen minimum zone waters. *Proceedings of the National Academy of Sciences* **113**, 10601–10606 (2016).

16. Kraft, B. *et al.* Oxygen and nitrogen production by an ammonia-oxidizing archaeon. *Science (1979)* **375**, 97–100 (2022).

17. Kalvelage, T. *et al.* Nitrogen cycling driven by organic matter export in the South Pacific oxygen minimum zone. *Nat Geosci* **6**, 228–234 (2013).

18. Peng, X. *et al.* Revisiting nitrification in the Eastern Tropical South Pacific: A focus on controls. *J Geophys Res Oceans* **121**, 1667–1684 (2016).

19. Zakem, E. J., Mahadevan, A., Lauderdale, J. M. & Follows, M. J. Stable aerobic and anaerobic coexistence in anoxic marine zones. *ISME J* **14**, 288–301 (2020).

20. Kalvelage, T. *et al.* Aerobic Microbial Respiration In Oceanic Oxygen Minimum Zones. *PLoS One* **10**, e0133526 (2015).

21. Garcia-Robledo, E. *et al.* Cryptic oxygen cycling in anoxic marine zones. *Proc Natl Acad Sci U S A* **114**, 8319–8324 (2017).

22. Zakem, E. J. & Follows, M. J. A theoretical basis for a nanomolar critical oxygen concentration. *Limnol Oceanogr* **62**, 795–805 (2017).

23. Margolskee, A., Frenzel, H., Emerson, S. & Deutsch, C. Ventilation Pathways for the North Pacific Oxygen Deficient Zone. *Global Biogeochem Cycles* **33**, 875–890 (2019).

24. Thamdrup, B., Dalsgaard, T. & Revsbech, N. P. Widespread functional anoxia in the oxygen minimum zone of the Eastern South Pacific. *Deep Sea Research Part I: Oceanographic Research Papers* **65**, 36–45 (2012).

25. Tiano, L. *et al.* Oxygen distribution and aerobic respiration in the north and south eastern tropical Pacific oxygen minimum zones. *Deep Sea Research Part I: Oceanographic Research Papers* **94**, 173–183 (2014).

26. Bristow, L. A. *et al.* N2 production rates limited by nitrite availability in the Bay of Bengal oxygen minimum zone. *Nat Geosci* **10**, 24–29 (2017).

27. Litchman, E. & Klausmeier, C. A. Competition of Phytoplankton under Fluctuating Light. *Am Nat* **157**, 170–187 (2001).

28. Kwiecinski, J. v. & Babbin, A. R. A High□Resolution Atlas of the Eastern Tropical Pacific Oxygen Deficient Zones. *Global Biogeochem Cycles* **35**, (2021).

29. Bayer, B., McBeain, K., Carlson, C. A. & Santoro, A. E. Carbon content, carbon fixation yield and dissolved organic carbon release from diverse marine nitrifiers. *Limnol Oceanogr* (2022) doi:10.1002/lno.12252.

30. Babbin, A. R., Keil, R. G., Devol, A. H. & Ward, B. B. Organic Matter Stoichiometry, Flux, and Oxygen Control Nitrogen Loss in the Ocean. *Science (1979)* **344**, 406–408 (2014).

31. Sun, X. *et al.* Uncultured Nitrospina-like species are major nitrite oxidizing bacteria in oxygen minimum zones. *ISME J* **13**, 2391–2402 (2019).

32. Sun, X., Ji, Q., Jayakumar, A. & Ward, B. B. Dependence of nitrite oxidation on nitrite and oxygen in low□oxygen seawater. *Geophys Res Lett* **44**, 7883–7891 (2017).

33. Füssel, J. *et al.* Adaptability as the key to success for the ubiquitous marine nitrite oxidizer *Nitrococcus*. *Sci Adv* **3**, (2017).

34. Weissman, J. L., Hou, S. & Fuhrman, J. A. Estimating maximal microbial growth rates from cultures, metagenomes, and single cells via codon usage patterns. *Proceedings of the National Academy of Sciences* **118**, (2021).

35. Lücker, S., Nowka, B., Rattei, T., Spieck, E. & Daims, H. The Genome of Nitrospina gracilis Illuminates the Metabolism and Evolution of the Major Marine Nitrite Oxidizer. *Front Microbiol* **4**, 1–19 (2013).

36. Connell, J. H. Diversity in Tropical Rain Forests and Coral Reefs. *Science (1979)* **199**, 1302–1310 (1978).

37. Li, W. K. W. Macroecological patterns of phytoplankton in the northwestern North Atlantic Ocean. *Nature* **419**, 154–157 (2002).

38. Jentsch, A. & White, P. A theory of pulse dynamics and disturbance in ecology. *Ecology* **100**, 1–15 (2019).

39. Lévy, M., Resplandy, L., Palter, J. B., Couespel, D. & Lachkar, Z. The crucial contribution of mixing to present and future ocean oxygen distribution. in *Ocean Mixing* (eds. Naveira-Garabato, A. C. & Meredith, M. P.) (2021).

40. Busecke, J. J. M., Resplandy, L. & Dunne, J. P. The Equatorial Undercurrent and the Oxygen Minimum Zone in the Pacific. *Geophys Res Lett* **46**, 6716–6725 (2019).

41. Tilman, D., Kilham, S. S. & Kilham, P. *Phytoplankton Community Ecology: The Role of Limiting Nutrients*. *Source: Annual Review of Ecology and Systematics* vol. 13 https://www.jstor.org/stable/2097072?seq=1&cid=pdf- (1982).

42. Seemann, T. Prokka: rapid prokaryotic genome annotation. *Bioinformatics* **30**, 2068–2069 (2014).

43. Weissman, J. L., Peras, M., Barnum, T. P. & Fuhrman, J. A. Benchmarking Community-Wide Estimates of Growth Potential from Metagenomes Using Codon Usage Statistics. *mSystems* **7**, (2022).

44. Aumont, O., Ethé, C., Tagliabue, A., Bopp, L. & Gehlen, M. PISCES-v2: an ocean biogeochemical model for carbon and ecosystem studies. *Geosci Model Dev* **8**, 2465–2513 (2015).

45. Tsujino, H. *et al*. JRA-55 based surface dataset for driving ocean–sea-ice models (JRA55-do). *Ocean Model (Oxf)* **130**, 79–139 (2018).

46. Locarnini, R. A. *et al. World Ocean Atlas 2018, Volume 1: Temperature*. *NOAA Atlas NESDIS 81* vol. 1 (2018).

47. Zweng, M. M. *et al. World Ocean Atlas 2018, Volume 2: Salinity*. *NOAA Atlas NESDIS 82* vol. 2 (2018).

48. Garcia, H. E. *et al*. World Ocean Atlas 2018, Volume 3: Dissolved Oxygen, Apparent Oxygen Utilization, and Oxygen Saturation. *NOAA Atlas NESDIS* **3**, 38 pp. (2019).

49. Garcia, H. E. *et al. World Ocean Atlas 2018. Volume 4: Dissolved Inorganic Nutrients (phosphate, nitrate and nitrate+nitrite, silicate). NOAA Atlas NESDIS 84* vol. 2 (2019).

50. Lauvset, S. K. *et al.* A new global interior ocean mapped climatology: the 1° × 1° GLODAP version 2. *Earth Syst Sci Data* **8**, 325–340 (2016).

51. Zakem, E. J. *et al*. Controls on the relative abundances and rates of nitrifying microorganisms in the ocean. *Biogeosciences* **19**, 5401–5418 (2022).

Acknowledgements

Model simulations and development were undertaken on Barkla, part of the High-Performance Computing facilities at the University of Liverpool. The authors wish to acknowledge use of the Ferret program (http://ferret.pmel.noaa.gov/Ferret/), climate data operators (https://code.mpimet.mpg.de/projects/cdo/), NetCDF Operators (http://nco.sourceforge.net/), Python (www.python.org) and GIMP (https://www.gimp.org/) for the analysis and graphics in this paper. Thanks to Clara Fuchsman who shared data, and ongoing discussions with Elena Litchman and Chris Klausmier. XS was supported by a Simons Foundation postdoctoral fellowship in Marine Microbial Ecology.

Data and code availability

All data and code are freely available. The chemostat model, model output, data, and scripts to reproduce the figures can be downloaded at https://doi.org/10.5281/zenodo.7653737. The biogeochemical model code is maintained at https://github.com/pearseb/C1D_PISCES_bac.